Japanese Journal of Applied Physics
Vol. 44, No. 10, 2005, pp. 7260–7266
©2005 The Japan Society of Applied Physics

Junction Temperature in Ultraviolet Light-Emitting Diodes

Yangang XI[1,2], Thomas GESSMANN[1,3], Jingqun XI[1,2], Jong Kyu KIM[1,3], Jay M. SHAH[1,3], E. Fred SCHUBERT[1,2,3*], Arthur J. FISCHER[4], Mary H. CRAWFORD[4], Katherine H. A. BOGART[4] and Andrew A. ALLERMAN[4]

[1]*Future Chips Constellation, Rensselaer Polytechnic Institute, Troy, NY 12180, U.S.A.*
[2]*Department of Physics, Applied Physics, and Astronomy, Rensselaer Polytechnic Institute, Troy, NY 12180, U.S.A.*
[3]*Department of Electrical, Computer, and Systems Engineering, Rensselaer Polytechnic Institute, Troy, NY 12180, U.S.A.*
[4]*Compound Semiconductor Research Laboratory, Sandia National Laboratories, Albuquerque, NM 87185, U.S.A.*

(Received February 4, 2005; accepted April 10, 2005; published October 11, 2005)

The junction temperature and thermal resistance of AlGaN and GaInN ultraviolet (UV) light-emitting diodes (LEDs) emitting at 295 and 375 nm, respectively, are measured using the temperature coefficient of diode-forward voltage. An analysis of the experimental method reveals that the diode-forward voltage has a high accuracy of $\pm 3^{\circ}$C. A comprehensive theoretical model for the dependence of diode-forward voltage (V_f) on junction temperature (T_j) is developed taking into account the temperature dependence of the energy gap and the temperature coefficient of diode resistance. The difference between the junction voltage temperature coefficient (dV_j/dT) and the forward voltage temperature coefficient (dV_f/dT) is shown to be caused by diode series resistance. The data indicate that the n-type neutral regions are the dominant resistive element in deep-UV devices. A linear relationship between junction temperature and current is found. Junction temperature is also measured by the emission-peak-shift method. The high-energy slope of the spectrum is explored in the measurement of carrier temperature. [DOI: 10.1143/JJAP.44.7260]

KEYWORDS: junction temperature, UV LEDs, AlGaN, temperature coefficient, diode-forward voltage, and thermal resistance

1. Introduction

III-V nitride semiconductors have a direct band gap and are thus very suitable for solid-state ultraviolet (UV) light sources. Such UV sources have a wide variety of applications, including those in UV-induced fluorescence, lighting, displays, photocatalytic processes, and high-resolution optics. Double-heterostructure GaInN/AlGaN UV light-emitting diodes (LEDs) emitting at 371 nm with an external quantum efficiency of 7.5% and an output power of 5 mW have been demonstrated.[1)] For deep-UV LEDs ($\lambda < 320$ nm), major goals are a short peak wavelength, a high efficiency, and a high output power. So far, AlGaN deep-UV LEDs with mW output power have been demonstrated.[2,3)] It was found, however, that the shorter the emission wavelength, the lower the device efficiency, indicating that junction heating problems are serious in deep-UV LEDs. Junction temperature is a critical parameter that affects internal quantum efficiency, external efficiency, maximum output power, and reliability. Hence, it is very important to accurately evaluate the junction temperature and thermal resistance of UV devices. Several groups have reported the measurement of the junction temperature of LEDs and laser diodes using micro-Raman spectroscopy,[4)] threshold voltage,[5)] thermal resistance,[6)] photothermal reflectance microscopy (PRM),[7)] electroluminescence (EL),[8)] photoluminescence (PL),[9)] a noncontact method[10)] and by using a nematic liquid crystal with infrared (IR) laser illumination.[11)] However, Raman spectroscopy needs a sophisticated experimental setup and has a limited accuracy; the threshold-voltage method and PRM are not applicable to LEDs; EL and PL methods are also limited in accuracy; the noncontact method[10)] uses the emission peak ratio of a dichromatic LED and thus can not be used for monochromatic LEDs.

In this study, diode-forward voltage is employed in the measurement of the junction temperature of UV LEDs with a high accuracy. A comprehensive analysis of the method and its application to UV LEDs are presented. The model takes into account the temperature coefficient of diode series resistance. The n-type neutral layer resistance is the dominant resistive factor in deep-UV LEDs. A linear relationship between junction temperature and current is found. Junction temperature is also measured by the emission-peak-shift method. The high-energy slope of the spectrum is explored in the measurement of the carrier temperature.

2. Theoretical Model of dV_f/dT

In order to derive the relationship between the forward voltage (V_f) of a diode and junction temperature, we start with the modified Shockley equation that includes a resistance term

$$J_f = J_s\left[\exp\left(\frac{eV_j}{n_{ideal}kT}\right) - 1\right] = J_s\left[\exp\left(\frac{eV_f - eAJ_fR_s}{n_{ideal}kT}\right) - 1\right], \quad (1)$$

where J_s is the saturation current density, V_j is the junction voltage, A is the area of the cross section of the device, R_s is the diode series resistance, and n_{ideal} is the diode ideality factor. The saturation current density, J_s, can be expressed as

$$J_s = e\left[\sqrt{\frac{D_n}{\tau_n}}\frac{n_i^2}{N_D} + \sqrt{\frac{D_p}{\tau_p}}\frac{n_i^2}{N_A}\right], \quad (2)$$

where D_n and D_p are the diffusion constants of electrons and holes, and τ_n and τ_p are the minority carrier lifetimes of electrons and holes, respectively. Both the diffusion constants and lifetimes are temperature-dependent. For phonon scattering, the diffusion constants decrease with temperature according to $T^{-1/2}$ dependence. The carrier lifetimes can

*E-mail address: efschubert@rpi.edu

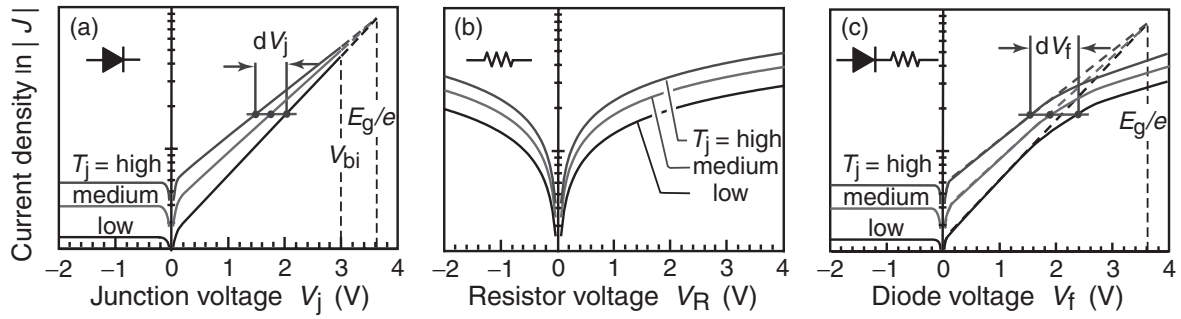

Fig. 1. (a) Schematic dependence of $\ln|J|$ on junction voltage V_j at low, medium and high temperatures. (b) *IV* of thermally activated series resistance. (c) Temperature dependence of forward voltage of resistive diode.

decrease (nonradiative recombination) or increase (radiative recombination) with temperature.

The intrinsic carrier concentration n_i, which depends exponentially on temperature, is given by

$$n_i = \sqrt{N_C N_V}\exp\left(-\frac{E_g}{2kT}\right), \tag{3}$$

where N_C and N_V are the effective densities of states at the conduction band and valence band edge, respectively. The conduction-band effective density of states is given by

$$N_C = 2\left(\frac{2\pi m_{de}kT}{h^2}\right)^{3/2} M_c \propto T^{3/2}, \tag{4}$$

where m_{de} is the density-of-state effective mass for electrons. M_c is the number of equivalent minima in the conduction band. For the valence-band density of states, N_C and m_{de} are replaced by N_V and m_{dh}, respectively, and $M_c = 1$.

Figure 1(a) shows the dependence of $\ln|J|$ on junction voltage V_j at different junction temperatures. An inspection of Fig. 1(a) shows that, at a constant current density, junction voltage decreases with increasing temperature. Figures 1(b) and 1(c) show the effect of series resistance. An inspection of voltage changes at the same current in Figs. 1(a) and 1(c), shows that series resistance increases the temperature coefficient of forward voltage. Thus, for UV LEDs, which typically have a large series resistance, the temperature coefficient of resistance must be taken into account.

For $V_f \gg kT/e$, eq. (1) can be approximated by

$$J_f = J_s\exp\left(\frac{eV_f - eAJ_fR_s}{n_{ideal}kT}\right). \tag{5}$$

Solving eq. (5) for the forward voltage yields

$$V_f = V_j + AJ_fR_s = \frac{n_{ideal}kT}{e}\ln\left(\frac{J_f}{J_s}\right) + AJ_fR_s. \tag{6}$$

In AlGaN deep-UV LEDs, series resistance is formed by either the p-type or the n-type neutral region. Let us arbitrarily assume that the dominant contribution is due to the p-type GaN layer. Then R_s can be written as

$$R_s = \rho\frac{L}{A} = \frac{1}{e\mu_p p}\frac{L}{A}. \tag{7}$$

Generally, μ_p is proportional to T^S,[12] where S has a typical value of $-1/2$ for phonon scattering. The carrier concentration p can be expressed as[13]

$$p \approx \left(\frac{1}{g}N_DN_C\right)^{1/2}\exp\left(-\frac{E_a}{2kT}\right), \tag{8}$$

where g is the ground-state degeneracy ($g = 2$ for donors and $g = 4$ for acceptors in GaN) and E_a is the acceptor activation energy. The derivative of forward voltage with respect to junction temperature for current I can then be written as

$$\begin{aligned}\frac{dV_f}{dT} &= \frac{dV_j}{dT} + AJ_f\frac{dR_s}{dT}\\ &= \frac{d}{dT}\left[\frac{n_{ideal}kT}{e}\ln\left(\frac{J_f}{J_s}\right)\right] + AJ_f\frac{dR_s}{dT}.\end{aligned} \tag{9}$$

We first consider the first term on the right-hand side of the equation. By substituting eqs. (3) and (4) into the first term, the temperature dependences of n_i, E_g, N_C, and N_V are taken into account. Executing the derivatives on the right-hand side of eq. (9) yields

$$\frac{dV_j}{dT} = \frac{eV_j - E_g}{eT} + \frac{1}{e}\frac{dE_g}{dT} - \frac{3k}{e}. \tag{10}$$

This equation gives the fundamental temperature dependence of junction voltage. The first summand on the right-hand side of the equation is due to the temperature dependence of intrinsic carrier concentration. The second summand is due to the temperature dependence of band-gap energy. Note that the second summand was not included in earlier derivations.[14] The contributions of this new term are about 24% for GaN, 29% for GaAs, and 15% for Si. The third summand, $3k/e$, is due to the temperature dependence of N_C and N_V. The inclusion of the temperature dependences of diffusion constants and lifetimes would only yield a minor contribution to the temperature coefficient ($< 5\%$ by calculation) and we therefore neglect these contributions. Light-emitting diodes are typically operated with their junction voltage close to the built-in voltage, i.e., $V_j \approx V_{bi}$. For nondegenerate doping concentrations, we can write

$$\begin{aligned}eV_j - E_g &\approx kT\ln\left(\frac{N_DN_A}{{n_i}^2}\right) - kT\ln\left(\frac{N_CN_V}{{n_i}^2}\right)\\ &= kT\ln\left(\frac{N_DN_A}{N_CN_V}\right).\end{aligned} \tag{11}$$

Furthermore, band-gap energy can be expressed as $E_g = E_0 - \alpha T^2/(\beta + T)$, where α and β are the Varshni parameters. For GaN,[15] $\alpha = 0.77\,\mathrm{meV/K^2}$, and $\beta = 600\,\mathrm{K}$. Substituting eq. (11) and Varshni parameters into eq. (10)

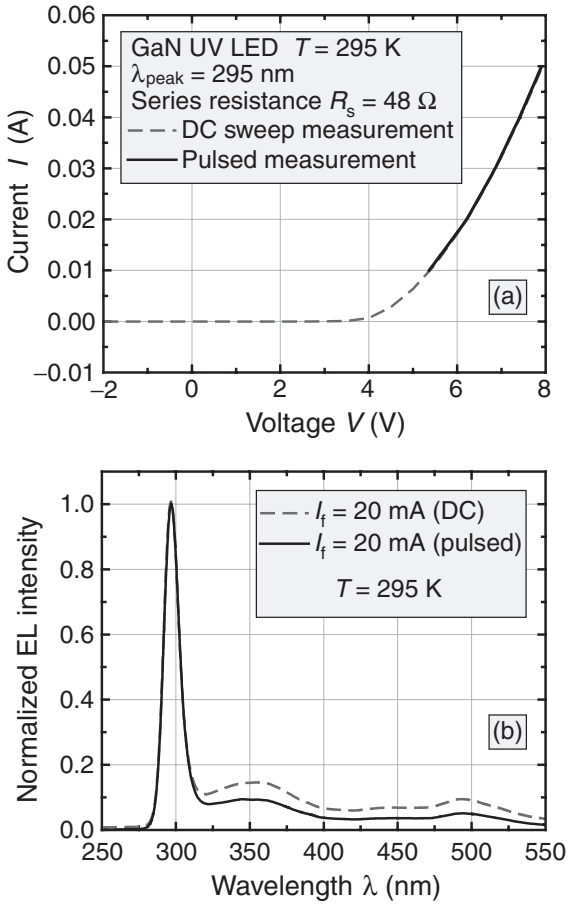

Fig. 2. (a) Current–voltage curve and (b) emission spectra under pulsed and DC conditions for AlGaN deep-UV LED.

yields

$$\frac{dV_j}{dT} \approx \frac{k}{e}\ln\left(\frac{N_D N_A}{N_C N_V}\right) - \frac{\alpha T(T+2\beta)}{e(T+\beta)^2} - \frac{3k}{e}. \quad (12)$$

This equation is a very useful expression for the temperature coefficient of junction voltage. Note that this expression is a *lower limit* for the magnitude of dV_j/dT, because the *junction voltage* is *less* than the *built-in voltage* in all practical cases. For GaN with $N_D = N_A = 2 \times 10^{16}\,\mathrm{cm}^{-3}$, one obtains $dV_j/dT = -1.76\,\mathrm{mV/K}$. For a Si p–n junction with the same doping concentration, one obtains $dV_j/dT = -1.74\,\mathrm{mV/K}$, which is in good agreement with that obtained by Millman and Halkias.[14)]

The derivative of series resistance with respect to junction temperature can be written as

$$\frac{dR_s}{dT} = \frac{L}{A}\frac{d}{dT}\left(\frac{1}{e\mu_p p}\right) = -\frac{1}{2}\frac{E_a + 2SkT}{kT^2}R_s. \quad (13)$$

The decrease in resistivity in the p-type GaN layer with increasing junction temperature was confirmed in a recent report.[16)] Substituting eqs. (10) and (13) into eq. (9), we obtain

$$\frac{dV_f}{dT} = \left(\frac{eV_j - E_g}{eT} + \frac{1}{e}\frac{dE_g}{dT} - \frac{3k}{e}\right)\Bigg|_{\text{due to junction}} - \left(\frac{1}{2}\frac{E_a + 2SkT}{kT^2}IR_s\right)\Bigg|_{\text{due to resistor}}. \quad (14)$$

Hence, dopant activation energy can be written as

$$E_a = \frac{2kT^2}{IR_s}\left(\frac{eV_j - E_g}{eT} + \frac{1}{e}\frac{dE_g}{dT} - \frac{3k}{e} - \frac{dV_f}{dT}\right) - 2SkT. \quad (15)$$

Since the experimental temperature coefficient of forward voltage is obtained by measurement, the theoretical temperature coefficient of junction voltage can be calculated by eq. (12) and the series resistance R_s can be measured, activation energy can be deduced from experimental data using eq. (15).

Although a good understanding of the temperature dependence of V_f has now been achieved, it is, due to a number of uncertainties, imperative that a calibration measurement of V_f as a function of T_j be performed. Thus, the forward-voltage method consists of two series of measurements, a calibration measurement and the actual junction-temperature measurement. In the calibration measurement, a pulsed forward current (with duty cycle 0.1%) drives the LED sample located in a temperature-controlled oven. The very small duty cycle ensures that the junction temperature is equal to the ambient temperature. An oscilloscope is used to measure the forward voltage V_f of the LED sample at different oven temperatures. The calibration measurement unequivocally establishes the relationship between forward voltage and junction temperature.

In the same calibration measurement, the emission peak energy is recorded, which allows one to deduce junction temperature from the shift of peak energy with temperature. The high-energy slope of the emission spectrum for a nondegenerate semiconductor follows the proportionality[17)]

$$I \propto \exp\left(-\frac{h\nu}{kT_c}\right), \quad (16)$$

where T_c is the *carrier temperature*. From eq. (16), we can get

$$\ln I = \text{const.} - \frac{h\nu}{kT_c}. \quad (17)$$

The derivative of $\ln I$ with respect to $h\nu$ can be expressed as

$$\frac{d\ln I}{dh\nu} = -\frac{1}{kT_c}. \quad (18)$$

Thus, the high-energy slope allows one to deduce the carrier temperature as a function of current.

3. Experimental Results and Discussion

To demonstrate the viability of the method, the junction temperatures of AlGaN deep-UV LEDs (Sandia National Labs., with a peak wavelength of 295 nm) and GaInN UV LEDs (Nichia Corp., with a peak wavelength of 375 nm) were determined. The 295 nm device is a 2×5 array of $0.3 \times 0.3\,\mathrm{mm}^2$ UV LEDs mounted in a TO-257 package. The device contains three-finger-interdigitated p and n electrodes to improve the current spreading. The multiple quantum-well active region of the LEDs consists of three periods of 20 Å $Al_{0.36}Ga_{0.64}N$ wells and 50 Å Si-doped $Al_{0.48}Ga_{0.52}N$ barriers.[3)] Figure 2(a) shows the *I–V* curve of the AlGaN/GaN LED sample under the pulsed current and DC conditions. The forward voltage at 20 mA is 6.24 V. The reverse breakdown voltage of the diode is 13.1 V. The electroluminescence spectrum displays a narrow, clean line with full-width at half-maximum (FWHM) of 11.6 nm

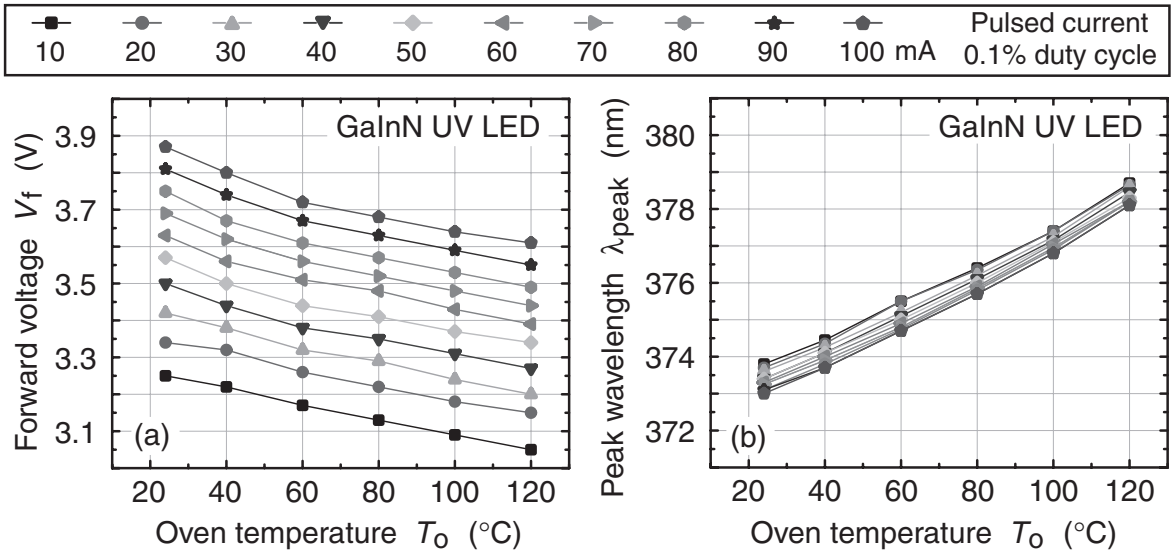

Fig. 3. (a) Experimental forward voltage and (b) peak position versus oven temperature for different pulsed injection currents in GaInN UV LEDs.

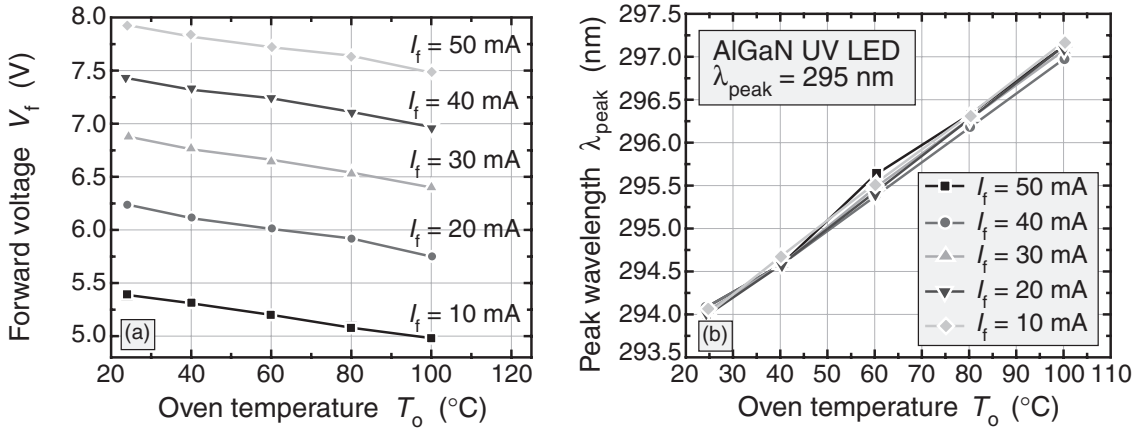

Fig. 4. (a) Experimental forward voltage and (b) peak position versus oven temperature for different pulsed injection currents in AlGaN deep-UV LEDs.

corresponding to $6.36\,kT$. The LED emission spectra for a forward current of $I_f = 20$ mA under DC and pulsed current conditions are shown in Fig. 2(b). The peak emission wavelength is 294.6 nm. A low-intensity below-band-gap transition is found at the long-wavelength part of the electroluminescence spectrum. It has been shown[3] that the intensity of the below-bandgap transition decreases with increasing injection current, consistent with the behavior of deep-level transitions.

For the 375 nm device, the pulsed current is increased, during the calibration measurement, from 10 to 110 mA in 10 mA increments. The measured forward-voltage-versus-junction-temperature relationship is shown in Fig. 3(a). Figure 3(b) shows the measured peak-position-versus-oven-temperature calibration results. From Fig. 3(a), the temperature coefficient of forward voltage at low currents is -2.3 mV/K, slightly larger in magnitude than the theoretical result of -1.76 mK/V. For the 295 nm device, during the calibration measurement, the pulsed current is increased from 10 to 50 mA in 10 mA increments. The measured forward-voltage-versus-oven-temperature relationship is shown in Fig. 4(a). Figure 4(b) shows the measured peak-position-versus-oven-temperature calibration results. From Fig. 4(a), the experimental temperature coefficient is $dV_f/dT = -5.8$ mV/K. For $N_A = N_D = 10^{16}$ cm^{-3}, the value calculated from eq. (12) is -2.04 mV/K, which is smaller (in magnitude) than the experimental coefficient. The difference between the theoretical and experimental coefficients is attributed to the resistive contributions of the neutral regions that exhibit a higher doping activation at elevated temperatures. A higher doping activation increases the conductivity of the neutral regions, thereby decreasing V_f.

Employing the experimental data discussed above, activation energy can be evaluated using eq. (15). In our GaN case, $R_s \approx 5\,\Omega$, $I = 20$ mA, $dV_f/dT = -2.3$ mV/K, and $dV_j/dT = -1.7$ mV/K. If we set $S = -1/2$, E_a is equal to 120 meV. For the AlGaN LEDs investigated here, $R_s \approx 48\,\Omega$, $I = 20$ mA, $dV_f/dT = -5.8$ mV/K, $dV_j/dT = -2.04$ mV/K, and E_a is equal to 100 meV. These values are in very good agreement with the Si donor activation energy that has been reported to be 86 meV in $Al_{0.50}Ga_{0.50}N$.[18] This suggests that the n-type resistance is the dominant contrib-

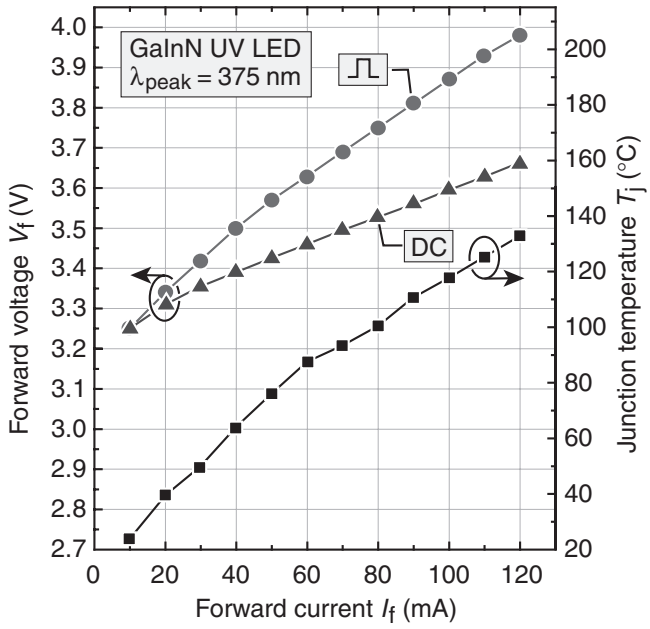

Fig. 5. Junction temperature versus forward current for GaInN UV LEDs. Also shown is the difference between DC and pulsed forward voltages.

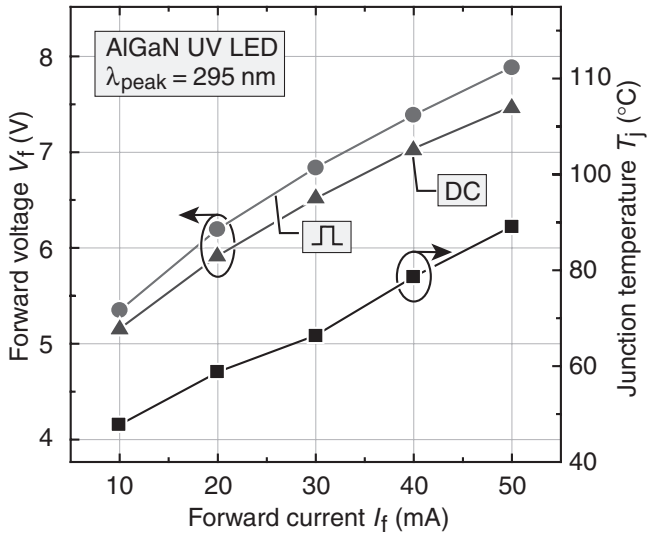

Fig. 6. Junction temperature versus DC current for AlGaN deep UV LEDs. Also shown is the difference between DC and pulsed forward voltage.

utor to the series resistance in AlGaN UV LEDs. The Mg acceptor activation energy is about 200 meV in GaN and even higher in AlGaN, i.e., much higher than the value extracted in our experiments.

Figure 5 shows junction temperature versus DC forward current determined using diode-forward voltage for GaInN UV LEDs. DC and pulsed voltages are also shown in the same figure. The difference between DC and pulsed voltages is due to the heating of the device under DC injection conditions. Figure 6 shows junction temperature, DC and pulsed voltages versus the forward current for AlGaN deep-UV LEDs. Junction temperature versus DC forward current for GaInN UV LEDs determined using the emission peak shift method is shown in Fig. 7. For comparison, the forward-voltage result is also shown in the same figure.

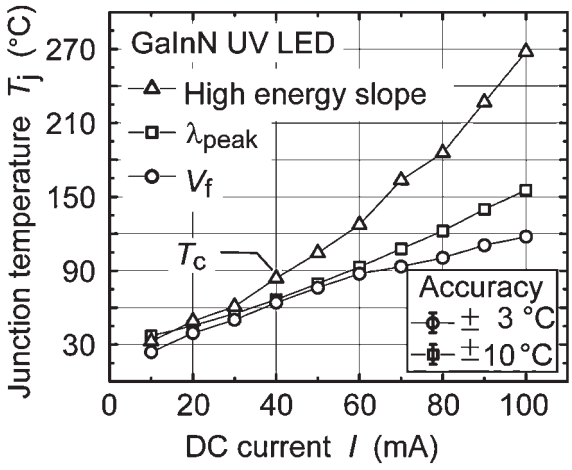

Fig. 7. Junction temperature versus DC current for GaInN UV LEDs.

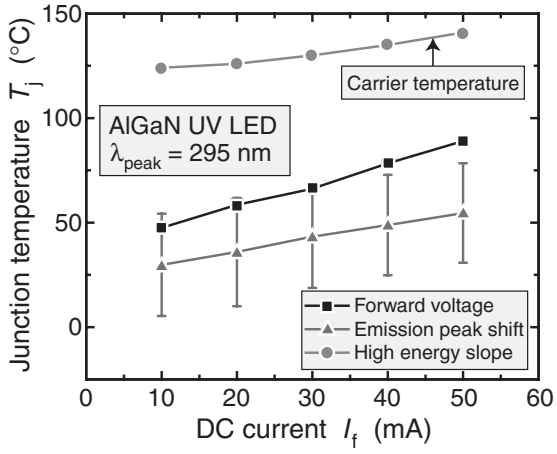

Fig. 8. Junction temperature versus DC current for AlGaN deep-UV LEDs.

Both T_j-vs-I_f curves shown in the figures are approximately linear. The linear fits of these curves are shown in the same diagram. A linear relationship between junction temperature and forward current has also been found for laser diodes.[19] In Fig. 7, as the DC forward current increases from 10 to 110 mA, the junction temperature obtained by measuring diode-forward voltage increases from 23 to 126°C. Figure 8 shows junction temperature versus the DC forward current determined using diode-forward voltage and emission peak shift for AlGaN deep-UV LEDs. In Fig. 8, the junction temperatures range between 43 and 87°C when the DC forward current increases from 10 to 50 mA. The junction temperature obtained by measuring diode-forward voltage is the most sensitive and its accuracy is estimated to be ±3°C.

Junction temperature determined from the emission peak energy shift is less accurate than that determined by the forward-voltage method due to the broad spectral width of the emission spectra. It is commonly accepted that the accuracy of peak energy is about 10% of the emission linewidth. If the error bar caused by the uncertainty in peak position (±24°C for AlGaN, ±10°C for GaInN) and the error bar of the forward-voltage measurement (±3°C) are taken into account, the first two methods are in good agreement. The temperature measured by the high-energy

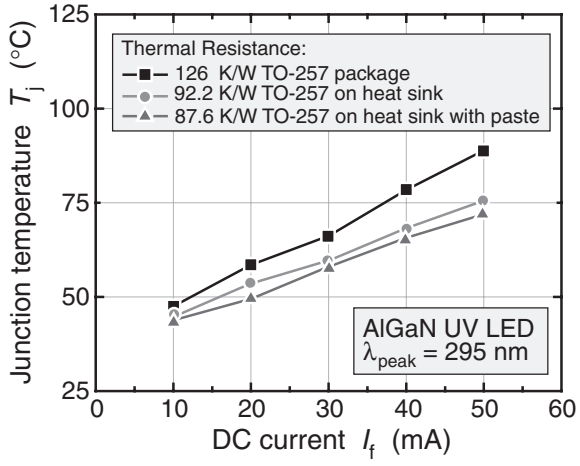

Fig. 9. Junction temperature as a function of DC current for AlGaN deep-UV LED between different packaging conditions.

slope method is the *carrier temperature*, which is higher than the lattice temperature at the junction. The high carrier temperature is likely caused by the injection of carriers from the high-energy barriers into the quantum wells. Furthermore, the broadening of the emission spectra due to unavoidable alloy composition fluctuations (alloy broadening) in the AlGaN and GaInN active regions can increase the linewidth, decrease the high-energy slope, and thereby increase apparent carrier temperature.

In order to reduce the thermal resistance of the AlGaN sample, several experiments were conducted with different heat sinks. Three different curves are shown in Fig. 9 along with their thermal resistances. The top curve corresponds to the packaged device, the middle curve corresponds to the device screwed onto a heat sink (a large heat sink with fins) and the bottom curve corresponds to the packaged device mounted on the heat sink with thermal paste. Commonwealth Scientific thermal paste, as used in microelectronics applications, was employed. The thermal resistance is 87.6 K/W for the device mounted on the heat sink with thermal paste.

Figure 10 shows junction temperature as a function of diode power, $I_f V_f$. An inspection of the figure reveals that this dependence is also approximately linear. From the slopes of the fitted curves, the thermal resistances of 342.2 K/W for the 375 nm device and 87.6 K/W for the 295 nm device are obtained.

Next, we explain the linear relationship between junction temperature and DC forward current. According to thermodynamics, heat transfers from a high-temperature object to a low-temperature object if they come into contact. It is well known that the conduction rate P_{cond} (heat energy transferred per unit time) is proportional to the temperature difference between the two objects

$$\Delta T \propto P_{cond}. \tag{19}$$

Under steady-state conditions, diode electric input power is (i) converted to light, (ii) consumed by unavoidable nonradiative recombination, and (iii) consumed by series resistance. Heat will be generated due to nonradiative recombination and series resistance. Thus, the electrical power P has two parts: P_l, converted to light and P_d,

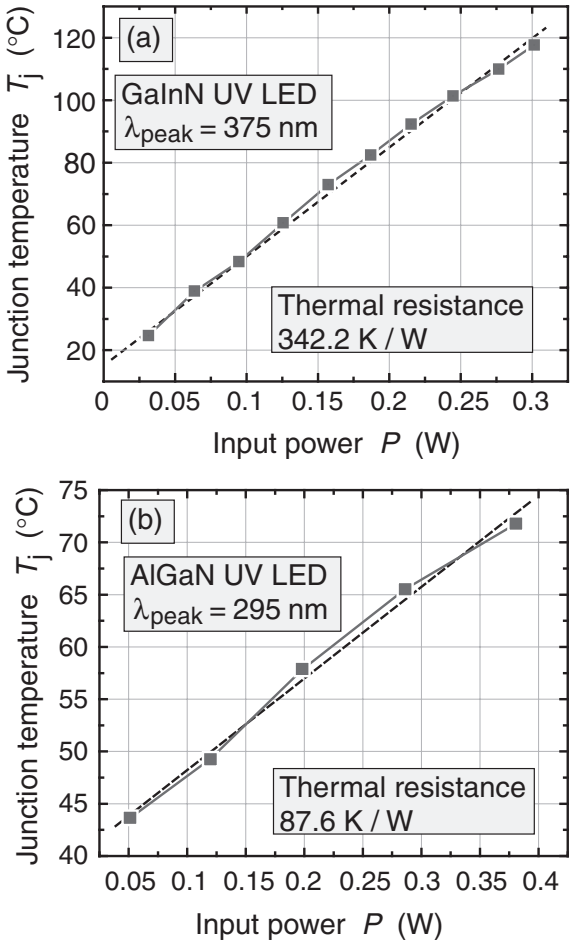

Fig. 10. Junction temperature versus diode power for two LEDs. Also shown is a linear fit for experimental data (dashed line).

dissipated power, converted to heat. In the steady state, dissipated power is equal to conduction rate. The total power is thus given by

$$P = P_d + P_l = I_f V_f = I_f(V_j + I_f R_s). \tag{20}$$

P_l can be expressed as

$$P_l = \eta I_f(V_f - I_f R_s), \tag{21}$$

where η is the external quantum efficiency. η is typically only 3–4% for deep UV LEDs. Using eqs. (20) and (21), we can obtain

$$P_d = P_{cond} = P - P_l = (1-\eta) I_f V_f + \eta I_f^2 R_s. \tag{22}$$

Since I_f is less than 120 mA, and $\eta \ll 1$, $\eta I_f^2 R_s$ can be neglected. Substituting eq. (22) into eq. (19) yields

$$\Delta T = T_j - T_a \propto I_f V_f, \tag{23}$$

where T_a is the ambient temperature. Because the changes in V_f with current are much smaller than V_f (i.e., $\Delta V_f \ll V_f$), eq. (23) indicates that junction temperature depends linearly on forward current. This is indeed found in our experiments, as shown in Fig. 10.

4. Conclusions

The junction temperature and thermal resistance of AlGaN and GaInN UV LEDs emitting at 295 and 375 nm, respectively, were measured using the temperature coeffi-

cient of diode-forward voltage. The analysis of the experimental method revealed that the measurement using diode-forward voltage has a high accuracy of $\pm 3^{\circ}$C. A comprehensive theoretical model for the dependence of diode-forward voltage (V_f) on junction temperature (T_j) was developed, taking into account the temperature dependence of the energy gap and the temperature coefficient of diode resistance. The difference between the junction voltage temperature coefficient (dV_j/dT) and the forward voltage temperature coefficient (dV_f/dT) was presented and explained. For the 295 nm device, the dopant activation energy extracted from the measurement was 100 meV, which is in good agreement with the activation energy of n-type $Al_{0.5}Ga_{0.5}N$. This indicates that the n-type neutral regions are the dominant resistive elements in deep-UV devices. A linear relationship between junction temperature and current was found. Junction temperature was also measured by the emission peak shift method. The high-energy slope of the spectrum was used in the measurement of carrier temperature. The thermal resistance of the AlGaN sample mounted on a heat sink with thermal paste was 87.6 K/W.

Acknowledgements

The support received at Rensselaer through the Defense Advanced Research Project Agency's (DARPA) Semiconductor Ultraviolet Optical Sources (SUVOS) program, the Army Research Office (ARO), the Samsung Advanced Institute of Technology (SAIT, Korea), Crystal IS, and the National Science Foundation (NSF) is gratefully acknowledged. Sandia is a multiprogram laboratory operated by Sandia Corporation for the United States DOE's National Nuclear Security Administration under Contract DE-AC04-94AL85000. Work at Sandia is supported by DARPA under the SUVOS program.

1) T. Mukai, D. Morita and S. Nakamura: J. Cryst. Growth **189–190** (1998) 778.
2) S. Wu, V. Adivarahan, M. Shatalov, A. Chitnis, W. H. Sun and M. Asif Khan: Jpn. J. Appl. Phys. **43** (2004) L1035.
3) A. J. Fischer, A. A. Allerman, M. H. Crawford, K. H. A. Bogart, S. R. Lee, R. J. Kaplar, W. W. Chow, S. R. Kurtz, K. W. Fullmer and J. J. Figiel: Appl. Phys. Lett. **84** (2004) 3394.
4) S. Todoroki, M. Sawai and K. Aiki: J. Appl. Phys. **58** (1985) 1124.
5) H. I. Abdelkader, H. H. Hausien and J. D. Martin: Rev. Sci. Instrum. **63** (1992) 2004.
6) S. Murata and H. Nakada: J. Appl. Phys. **72** (1992) 2514.
7) P. W. Epperlein: in *Proc. 17th Int. Symp. of Gallium Arsenide and Related Compounds* (IOPP, Bristol, 1990) Inst. Phys. Conf. Ser., No. 112, p. 633.
8) P. W. Epperlein and G. L. Bona: Appl. Phys. Lett. **62** (1993) 3074.
9) D. C. Hall, L. Goldberg and D. Mehuys: Appl. Phys. Lett. **61** (1992) 384.
10) Y. Gu and N. Narendran: Proc. SPIE **5187** (2004) 107.
11) J. Park, M. Shin and C. C. Lee: Opt. Lett. **29** (2004) 2656.
12) M. Rubin, N. Newman, J. S. Chan, T. C. Fu and J. T. Ross: Appl. Phys. Lett. **64** (1994) 64.
13) E. F. Schubert: *Doping in III–V Semiconductors* (Cambridge University Press, Cambridge, U.K., 1993).
14) J. Millman and C. Halkias: *Integrated Electronics* (McGraw-Hill, New York, 1972).
15) http://www.ioffe.rssi.ru/SVA/NSM/Semicond/
16) J. Kwak, O. Nam and Y. Park: J. Appl. Phys. **95** (2004) 5917.
17) E. F. Schubert: *Light Emitting Diodes* (Cambridge University Press, Cambridge, U.K., 2003).
18) J. M. Rommel, P. Gavrilovic and F. P. Dabkowski: J. Appl. Phys. **80** (1996) 6547.
19) J. Y. Lin and H. X. Jiang: Proc. SPIE **4999** (2003) 287.